

# Vertical distribution of near-ground aerosol backscattering coefficient measured by a CCD side-scattering lidar

Zongming Tao<sup>1,2</sup> · Dong Liu<sup>2</sup> · Xiaomin Ma<sup>1</sup> · Bo Shi<sup>1</sup> · Huihui Shan<sup>1</sup> · Ming Zhao<sup>2</sup> · Chenbo Xie<sup>2</sup> · Yingjian Wang<sup>2,3</sup>

Received: 14 January 2015 / Accepted: 9 July 2015 / Published online: 21 July 2015  
© Springer-Verlag Berlin Heidelberg 2015

**Abstract** The near-ground aerosols have the most impact on the human beings. Its fine spatial and temporal distribution, with which the environmental and meteorological departments concern themselves most, has not been elaborated very well due to the unavailable measurement tools. We present the continuous observations of the vertical profile of near-ground aerosol backscattering coefficients by employing our self-developed side-scattering lidar system based on charge-coupled device camera. During the experimental period from April 2013 to August 2014, four catalogs of aerosol backscattering coefficient profiles are found in the near ground. The continuous measurement is revealed by the contour plots measured during the whole night. These experimental results indicate that the aerosol backscattering coefficients in near ground are inhomogeneous and vary with altitude and time, which are very useful for the model researchers to study the regional air pollution and its climate impact.

## 1 Introduction

Aerosol is one of the sources which deteriorate the air quality. Air pollution often happens in a layer of a few

kilometers from ground, generally called the planetary boundary layer. Aerosol monitoring, especially on its vertical structures, is needed for the air pollution control. Right now, remote sensing techniques enabled by a variety of instruments have been applied to detect aerosol vertical distribution, and the main tool is the backscattering lidar providing range-resolved atmospheric profiles continuously [1, 2]. But the common backscattering lidar system has a shortcoming in the lower hundreds of meters because of the geometric form factor caused by the configuration of the transmitter divergence and receiver's field-of-view (FOV) at the near range [3]. The geometric form factor can be derived by horizontal-pointing measurement of a lidar system. For the vertical fixed lidar system, the Raman technique can be adopted. The aerosol vertical distribution in near ground is very important and attracts the attention of the environmental and meteorological department, but the traditional lidar needs the correction of the geometric form factor which could cause additional errors.

Our side-scattering lidar (S-lidar) based on charge-coupled device (CCD) detector is a developing technique in which the CCD camera is set to look the laser beam in a certain distance [4]. Compared with the backscattering lidar, there are four different aspects: (1) using side-scattering instead of backscattering light, (2) receiving signals without range square dependence, (3) variable vertical altitude resolution, and the closer to the surface, the better resolution, and (4) no overlap issues. With overlap problem solved, the side-scattering lidar is especially suitable to detect aerosol vertical profile in the near range [5–7]. The fundamental principle and key techniques including the retrieval and validation of the aerosol phase function and backscattering coefficient profiles measured by a CCD side-scattering lidar have been described in the previous work [7]. This paper focuses on the observational results

---

✉ Dong Liu  
dliu@aiofm.cas.cn

<sup>1</sup> Department of Basic Sciences, Army Officer Academy, Hefei 230031, China

<sup>2</sup> Key Laboratory of Atmospheric Composition and Optical Radiation, Anhui Institute of Optics and Fine Mechanics, Chinese Academy of Sciences, Hefei 230031, China

<sup>3</sup> University of Science and Technology of China, Hefei 230026, China

of near-range aerosol vertical profile patterns and new findings based on more than 1-year experiments.

## 2 System and methods

Side-scattering lidar system consists of laser, CCD camera, geometric calibration, and data acquisition units. The diagram of a S-lidar is shown in Fig. 1. Side-scattering signals are recorded by CCD, with each pixel recording a side-scattering signal at its corresponding altitude. For the S-lidar, the received laser power scattered by the aerosol then can be written as [5]

$$P(\theta) = \frac{P_0KA}{D} \beta(\theta) T_z T_r d\theta \quad (1)$$

where  $P(\theta)$  is the received photon number at altitude  $z$  and scattering angle  $\theta$  by a pixel,  $P_0$  is the photon number emitted by laser,  $A$  is the area of the CCD camera lens,  $K$  is a system constant,  $D$  is the distance from CCD to laser beam,  $T_z$  and  $T_r$  are the molecular and aerosol atmospheric transmittance from the laser to altitude  $z$  and from altitude  $z$  along the slant path to the CCD camera, respectively,  $\beta(\theta)$  is the molecular and aerosol side-scattering coefficient, and  $d\theta$  is the FOV of a pixel.

The main specifications of the S-lidar system are summarized in Table 1, and the detailed description is described in Ref. [7].

The vertical altitude resolution  $dz$  is described as

$$dz = \frac{D}{\sin^2 \theta} d\theta \quad (2)$$

From Fig. 1 and Eq. (2), one can know that the vertical altitude resolution is finer in lower altitude of the planetary boundary layer [5].

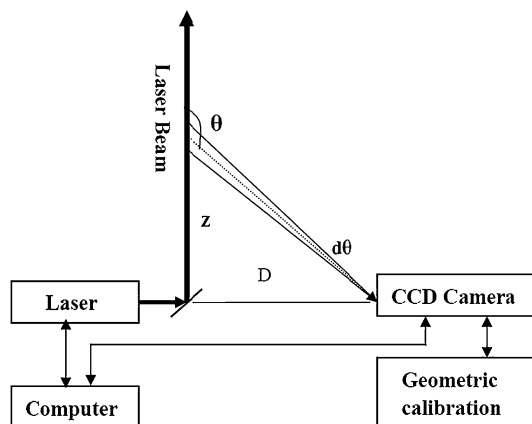


Fig. 1 Diagram of side-scattering lidar

Table 1 Main specifications of the side-scattering lidar system

Laser (Quantel Brilliant) Nd:YAG	
Wavelength (nm)	532
Pulse energy (mJ)	200
Repetition rate (Hz)	10
Detector (SBIG) ST-8300M	
Pixel array	3352 × 2532
Pixel size (μm)	5.4 × 5.4
A/D convector (bits)	16
Wide-angle lens	Walimexpro f/2.8
Lens focal length (mm)	14
CCD sensor (Kodak) KAF-8300	
Quantum efficiency (532 nm)	~55 %
Interference filter (Semrock corporation)	
Bandwidth (nm)	25.6
Peak transmittance	~95 %

Fernald provided an interactive inversion solution to backscattering lidar [8], but his method is not suitable to side-scattering lidar, due to the difference of the atmospheric transmittance and the adoption of the molecular and aerosol phase function. Using relative aerosol phase function  $f(\theta)$ , the S-lidar equation in backscattering ( $90^\circ \leq \theta \leq 180^\circ$ ) can be rewritten as

$$P(\theta) = \frac{P_0KA}{D} [\beta_a(\pi) f_a(\theta) + \beta_m(\pi) f_m(\theta)] \times \exp \left\{ - \int_0^z [\alpha_a(z') + \alpha_m(z')] dz' - \int_0^{z/\cos(\pi-\theta)} [\alpha_a(z') + \alpha_m(z')] dz' \right\} \times d\theta \quad (3)$$

where  $\beta_a(z)$  and  $\beta_m(z)$  are aerosol and molecule backscattering coefficients, respectively,  $f_a(\theta)$  and  $f_m(\theta)$  are relative aerosol and molecule phase function, respectively,  $\alpha_a(z)$  and  $\alpha_m(z)$  are aerosol and molecule extinction coefficients, respectively.

Generally, there are six unknown variables in Eq. (3), i.e., relative phase functions, backscattering and extinction coefficients for aerosol and molecule. Three molecular variables can be calculated in accordance with Rayleigh scatter theory and molecular model. A prior assumption has to be given; i.e., lidar ratio (extinction-to-backscatter ratio) of aerosol and the relative aerosol phase function is determined from skyradiometer (e.g., POM02) [9], and then only one variable (backscattering or extinction coefficient of aerosol) is left in Eq. (3).

In our experiment, vertical-pointing backscattering lidar (V-lidar) and S-lidar worked simultaneously. For V-lidar data processing, it is a traditional way to select the clear point about the tropopause as reference point

where assumed has minimum aerosol. The V-lidar signals and S-lidar signals have an overlap region around 1 km in height in our case. For S-lidar, the reference point is selected in this overlap region. Aerosol backscatter coefficient value at reference point thus can be given from V-lidar retrieval. When the aerosol backscatter coefficient value at the scattering angle  $\theta_c$  (as reference point) is known, according to Eq. (3), the backscattering or extinction coefficient of aerosol can be derived by our proposed numerical inversion method [7].

### 3 Validation and error analysis

In order to further validate the numerical inversion method proposed by us, comparative experiments were arranged as follows: Three lidars worked at same position simultaneously; one CCD side-scattering and one backscattering lidars worked vertically; another backscattering lidar worked horizontally. In the evening on October 22, 2013, the comparison experiments were performed. On that nighttime, it was clear sky with the minimum temperature of 10 °C near ground and southeast wind of not more than 5 m s<sup>-1</sup>. Figure 2 shows the validation results.

Figure 2 shows the retrieved aerosol backscattering coefficients by different lidars at 18:40 LST. The black solid lines in Fig. 2 are the retrieved aerosol backscatter coefficient profiles using V-lidar; the gray lines in Fig. 2 are the aerosol backscattering coefficient profiles from the S-lidar by our proposed method; the black star is the aerosol backscattering coefficient near the ground by the horizontal-pointing backscattering lidar (H-lidar).

From Fig. 2, one can see that between 0.6 and 1.4 km altitude, the aerosol backscattering coefficients measured by the side-scattering lidar and vertical-pointing backscattering lidar are in a good agreement. From the ground to about 0.6 km, the aerosol backscattering coefficient retrieved from V-lidar is not correct due to the overlap factor, so there is a big divergence between V-lidar and S-lidar results in this range. The S-lidar results have a good agreement with the H-lidar retrieval at 50 m above ground level (AGL). In practice, to avoid the obstructions, the laser beam has an elevation angle of 2° in the process of the horizontal measurement. The slant range corresponding to 50 m in vertical is about 1.5 km horizontally.

The errors of the backscattering coefficient retrieval from the CCD lidar were also examined. Error sources are from six unknown variables and uncertainties in Eq. (3), i.e., molecular backscattering coefficient, relative phase functions of molecule and aerosol, aerosol extinction–backscattering ratio, aerosol backscatter coefficient value at reference point and the received photon number.

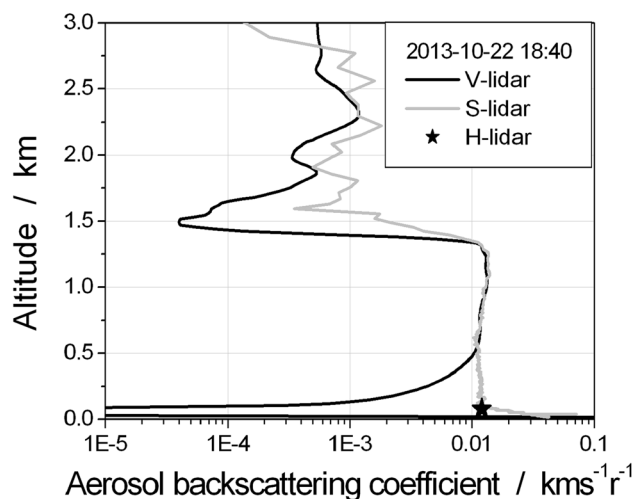


**Fig. 2** Retrieved profiles of aerosol backscattering coefficient by vertical-pointing backscattering lidar, side-scattering lidar and backscattering lidar pointing horizontally measured at 18:40 LST

Once changing one unknown variable independently, and applying the error propagation method, the error caused by this changing variable could be computed from Eq. (3). In this way, the individual error was computed first, and then, the total errors could be composed [10]. Taking the data in Fig. 2 as example, if the relative error of molecular backscattering coefficient is 5 %, the relative error from molecular relative phase function is 5 %; the relative error of the received photon number is 5 %; the relative error from aerosol relative phase function is 10 %; the relative error from aerosol backscatter coefficient value at reference point is 10 %; the relative error of aerosol extinction–backscattering ratio is 15 %; the total relative error of backscattering coefficient is less than 18 %.

### 4 Results

The measurements of near range aerosol vertical profiles were made during April 2013 through August 2014 with our self-developed side-scattering lidar in use. Aerosol lidar ratio is assumed as 50 Sr, and relative aerosol phase function is retrieved from POM02 sky radiometer at the same place and the same day. All the data have been analyzed to derive aerosol backscattering coefficient. After analyzing the experimental results, we found that aerosol backscattering coefficient is not uniform with altitude in near ground and can be classified into four categories. Figure 3 shows four typical cases acquired on August 3, 2014 (a), August 2, 2014 (b), July 10, 2014 (c) and August 15, 2013 (d).

On August 3, 2014, it was clear at night, with the minimum temperature of 26 °C near ground, southwest wind of not more than 5 m s<sup>-1</sup>. In Fig. 3a, the aerosol profile was

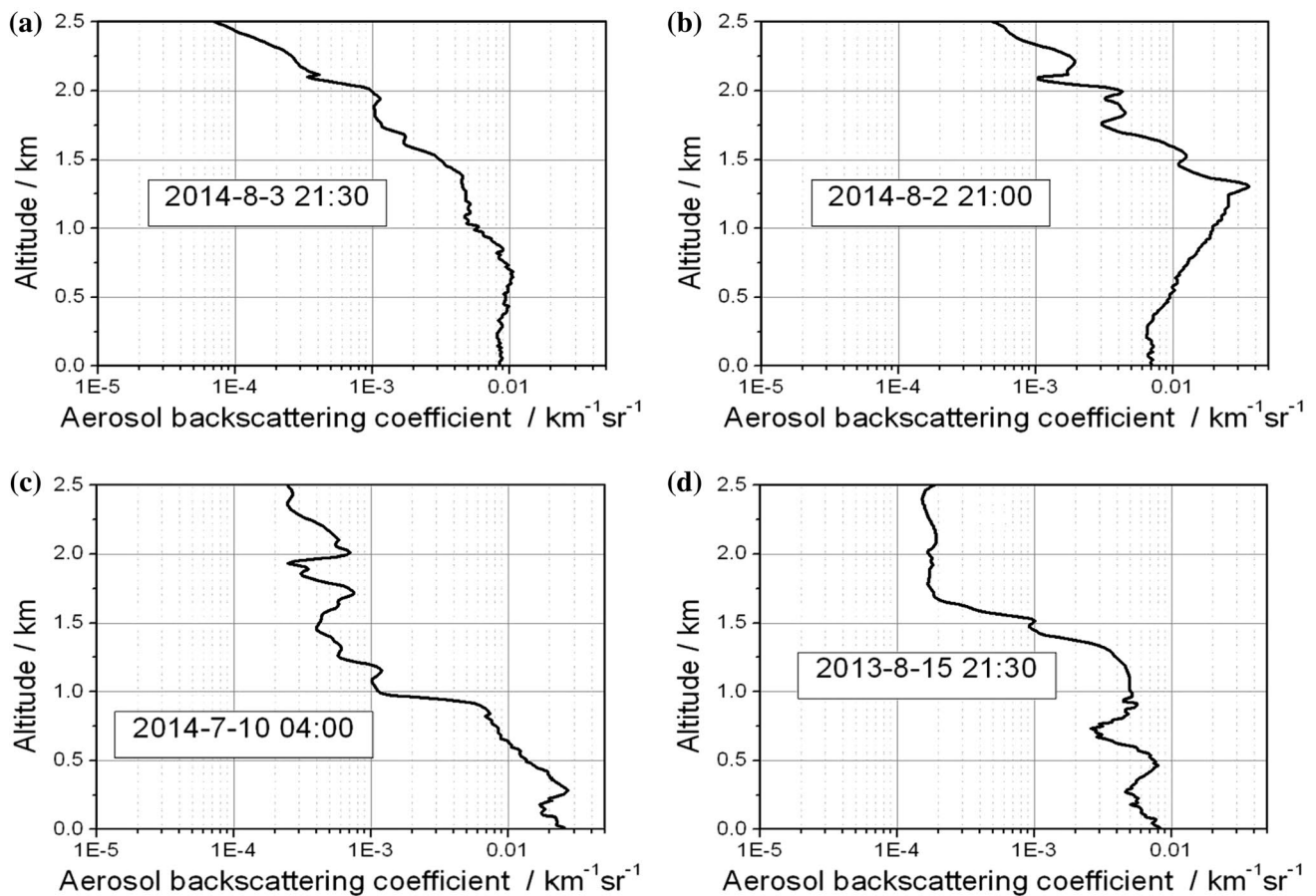


**Fig. 3** Four catalogs aerosol profiles, **a** acquired on August 3, 2014, at 21:30, **b** on August 2, 2014, at 21:00, **c** on July 10, 2014, at 4:00, **d** on August 15, 2013, at 21:30, respectively

measured at 21:30 Beijing time on August 3, 2014; the distance  $D$  between laser beam and CCD camera is 14.21 m. The aerosol backscattering coefficient approximately had a constant value  $0.009 \text{ km}^{-1} \text{ sr}^{-1}$  within 0.8 km. This means that the aerosol concentration kept almost constant within this range in this case, indicating the boundary layer was well mixed.

On August 2, 2014, it was clear at night, with the minimum temperature of  $26 \text{ }^\circ\text{C}$  near ground, west wind of not more than  $5 \text{ m s}^{-1}$ . In Fig. 3b, the aerosol profile was measured at 21:00 Beijing time on August 2, 2014; the distance  $D$  between laser beam and CCD camera is 8.83 m. The aerosol backscattering coefficient increased versus altitude from 0.007 to  $0.035 \text{ km}^{-1} \text{ sr}^{-1}$  within 1.3 km, which was quite exceptional compared with the normal exponential decreasing trend of the aerosol loading in planet boundary layer.

On July 10, 2014, it was cloudy at night, with the minimum temperature of  $25 \text{ }^\circ\text{C}$  near ground, south wind of not more than  $5 \text{ m s}^{-1}$ . In Fig. 3c, the aerosol profile was measured at 04:00 Beijing time on July 10, 2014; the distance

$D$  between laser beam and CCD camera is 9.23 m. The aerosol backscattering coefficient decreased from  $0.015$  to  $0.007 \text{ km}^{-1} \text{ sr}^{-1}$  within 0.8 km, indicating a good normal exponential decreasing trend. And also, one can find there is another inversion layer at the altitude of 200 m, which cannot be observed by the traditional backscattering lidar, highlighting the advantage of the CCD side-scattering lidar.

On August 15, 2014, it was cloudy at night, with the minimum temperature of  $21 \text{ }^\circ\text{C}$  near ground, southeast wind of not more than  $5 \text{ m s}^{-1}$ . In Fig. 3d, the aerosol profile was measured at 21:30 Beijing time on August 15, 2013; the distance  $D$  between laser beam and CCD camera is 11.50 m. The aerosol backscattering coefficient displayed multilayer structure within 1.4 km; the subpeaks are at ground, 0.5 and 1.0 km in altitude, demonstrating the complexity of the vertical aerosol distribution.

In order to show the continuous aerosol backscattering coefficient variation, Fig. 4 depicts two contour plots measured at summer night and autumn night, respectively. In Fig. 4a, aerosol profile was measured from 20:00 on July 9, 2014, to 05:00 on July 10, 2014, and the distance

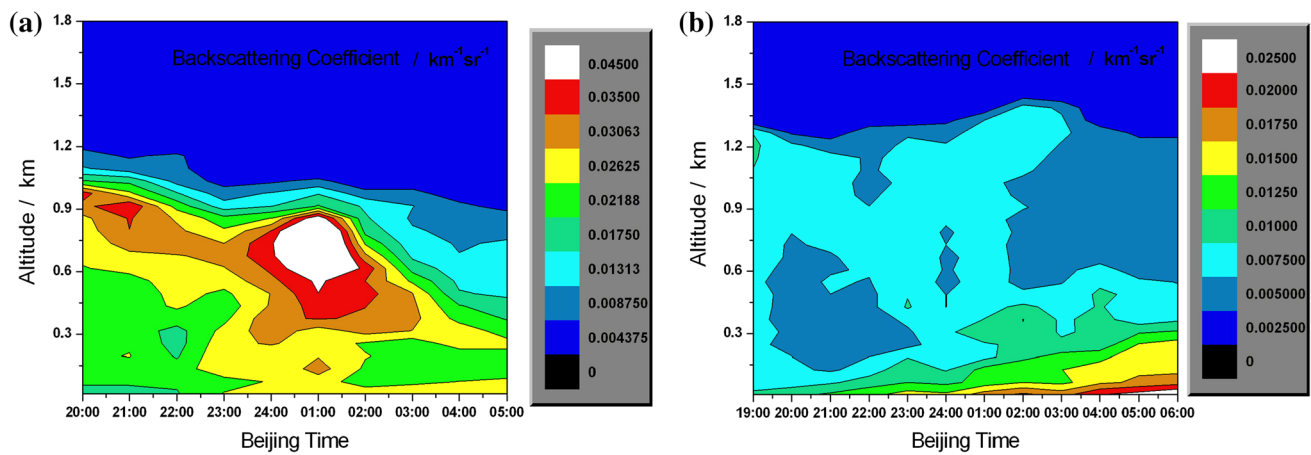


**Fig. 4** Continuous measurements of aerosol backscattering coefficient profiles, **a** measured from 20:00 on July 9, 2014, to 05:00 on July 10, 2014, **b** from 19:00 on October 8, 2014, to 06:00 on October 9, 2014

$D$  between laser beam and CCD camera is 9.22 m. During that period, it was cloudy, with the minimum temperature of 25 °C near ground, west wind of not more than 5 m s<sup>-1</sup>. From Fig. 4a, one can see that aerosol showed complex layered characteristic in nocturnal boundary layer, all layer descended versus time, and the height of the planetary boundary layer decreased from 1.2 to 0.9 km during the whole night. Around 1:00 a.m., between 0.5 and 0.9 km, the aerosol backscattering coefficient increases probably due to the change in the ambient meteorological conditions.

In Fig. 4b, aerosol profile was measured from 19:00 on October 8, 2013, to 05:30 on October 9, 2014, and the distance  $D$  between laser beam and CCD camera is 23.74 m. During that period, it was clear, with the minimum temperature of 26 °C near ground, east wind of not more than 5 m s<sup>-1</sup>. Figure 4b shows the residual layer within 1.30 km, changing slightly during the whole night. In near ground within 150 m in altitude, a surface layer formed and got thicker with time, reaching peak at 05:30.

## 5 Conclusions

In summary, our self-developed side-scattering lidar system could measure the profile of aerosol backscattering coefficient from ground, and the spatial and temporal variations of near-ground aerosol backscattering coefficients were obtained quantitatively. From the experimental results, one can find the near-ground aerosol backscattering coefficients

are inhomogeneous and change with altitude and time. Taking the advantage of the CCD side-scattering lidar, the fine resolution structures of the near-ground aerosol distribution could allow the molders to study the regional air pollution and assess the effect of the corresponding control measures.

**Acknowledgments** This work was supported by the National Natural Science Foundation of China under Grant Nos. 41175021 and 41005014 and China Special Fund for Meteorological Research in the Public Interest under Grant Nos. GYHY201106002-03 and GYHY201206037-09.

## References

1. D. Winker, W. Hunt, M. McGill, Res. Lett. **34**, L19803 (2007). doi:10.1029/2007GL30135
2. Z. Chen, W. Liu, Y. Zhang, N. Zhao, J. He, J. Ruan, Chin. Opt. Lett. **7**, 753–755 (2009)
3. S. Hu, X. Wang, Y. Wu, C. Li, H. Hu, Opt. Lett. **30**(14), 1879–1881 (2005)
4. X. Ma, Z. Tao, M. Ma, C. Li, Z. Wang, D. Liu, C. Xie, Y. Wang, Acta Opt. Sin. (2014). doi:10.3788/AOS201434.0201001
5. J.E. Barnes, S. Bronner, R. Beck, N.C. Parikh, Appl. Opt. **42**(15), 2647–2652 (2003)
6. J.E. Barnes, N.C. Parikh Sharma, T.B. Kaplan, Appl. Opt. **46**(15), 2922–2929 (2007)
7. Z. Tao, D. Liu, Z. Wang, X. Ma, Q. Zhang, C. Xie, S. Hu, Y. Wang, Opt. Express (2014). doi:10.1364/OE.22.001127
8. F.G. Fernald, Appl. Opt. **23**(5), 652–653 (1984)
9. T. Nakajima, G. Tonna, R. Rao, P. Boi, Y. Kaufman, B. Holben, Appl. Opt. **35**(15), 2672–2686 (1996)
10. Q. Zhang, Y. Chen, X. Ma, B. Shi, H. Shan, Z. Tao, Jiangxi Sci. **32**(3), 267–271 (2014)